

Tribocharging and Materials Analysis of Firearm Propellants

Daniel J. Breton, Emily Asenath-Smith, and Nathan J. Lamie
U.S. Army Cold Regions Research and Engineering Laboratory
72 Lyme Road, Hanover, NH USA
phone: +1 603-646-4197
e-mail: daniel.j.breton at usace.army.mil

Abstract—In this work, we studied tribocharging processes of an M9 Beretta pistol, firing three different types of ammunition. For the pistol shots, we recorded highly reproducible charge transients in the immediate vicinity of the muzzle, and subsequent transients measured 10 m downrange associated with passage of the charged projectile through two cylindrical charge sensors. The charge transients demonstrated both positive and negative charge components evolving over time, providing a unique signature for each type of ammunition used. Propellant residues were collected for material analysis. Electron microscopy and energy dispersive spectroscopy, were performed on the residues to determine particle sizes and composition.

I. INTRODUCTION

Tribocharging in very dynamic systems, such as those of projectiles launched from firearms, has been reported [1], [2] and prototype systems have been developed to detect the charge and relative position of these projectiles [3], [4], [5]. The focus of these works is on the *projectile charge* as this forms the technical basis for an electrostatic shot detection system.

However, the wide range of estimated projectile charges reported in [3] presents a practical problem: estimating the performance of and the probability of detection for such a system depends critically on correctly characterizing the projectile charge distribution. Shot detection presumably improves with larger magnitude projectile charges, but large magnitudes of charge appear to be relatively rare. The median projectile charge in [3] was reported to be 6.4 pC, suggesting a slight preference towards positive charges despite a range of well over ± 25 pC for the 135 recorded shots fired from five different weapon types.

In an attempt to better understand this wide variability, we conducted experiments using three different ammunition types fired through a single weapon, and conducted a materials analysis of both the unburned and burned propellant used in the ammunition.

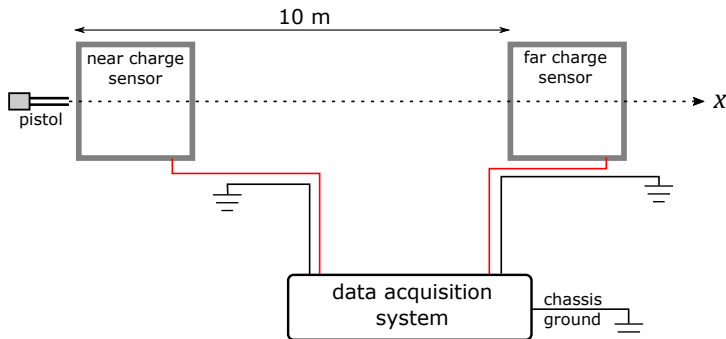


Fig. 1. Overhead view of testing setup at firing range showing relative locations of pistol, conductive mesh charge sensors and data acquisition system, a Picoscope 5444B. The sketch is not drawn to scale. Grounds shown are separate grounding stakes used in the vicinity of each charge sensor and at the data acquisition system.

II. MATERIALS AND METHODS

Experiments were performed at an outdoor shooting range using an M9 9 mm, Beretta pistol, two cylindrical conductive mesh sensors fabricated at our Laboratory, and a data acquisition system consisting of a laptop-operated Picoscope 5444B (1 M Ω input impedance, Picotech) oscilloscope sampling at 125 MHz, 14 bit resolution. A sketch of the setup is shown in Fig. 1 and a theoretical discussion of the conductive mesh sensors is given in [6].

Triggering of the recording system was achieved by a voltage threshold on the near charge sensor. No charge or voltage amplification was used on the conductive mesh sensors, and all equipment was battery powered to minimize electrical noise associated with portable electrical power generators. Despite this, a significant 60 Hz noise signal remains in the data, but was difficult to filter as the period of the signal of interest is unfortunately similar to that of the noise. The recorded signals were Savitzky-Golay [7] filtered to remove high frequency noise.

A. Ammunition

Three different types of 9 mm ammunition were purchased from the same manufacturer (Federal Premium Ammunition; Anoka, MN) and all rounds were fired through the same Beretta M9 9mm pistol:

- 115 grain Fully Metal Jacketed (FMJ), Load #AE9DP, 16 rounds
- 115 grain Metal Jacketed Hollow Point (JHP), Load #C9BP, 10 rounds
- 124 grain Metal Jacketed Hollow Point “HS” (JHP-HS), Load #P9HS1, 7 rounds.

The chemical and physical makeup of the primer and propellant powder within the rounds is proprietary, but we were able to confirm (personal communication, Federal Premium Ammunition) that the primer and propellant compositions were the same (within

manufacturing tolerances) for all three types of ammunition used. Projectile core and jacketing materials, as well as those for the cartridge itself, are also the same for all three ammunition types.

B. Materials Analysis

We obtained propellant grains from a 115 grain (7.45 g) FMJ cartridge to allow composition and particle size analysis for the propellant representative of that used in all of our firings. A sample of these grains were burned in an aluminum planchet with a propane torch to provide us with particulate material approximating that ejected from a firing weapon.

We used a Phenom XL scanning electron microscope (SEM) equipped with a energy dispersive spectroscopy (EDS) system to obtain micrographs and point EDS spectra of both unburned and burned propellant granules. Large particle samples were mounted on carbon tape, while smaller particulates were drop cast using ethanol as the carrier solvent onto a silicon wafer. No coating was used on any of our samples during imaging.

III. RESULTS

The results for each type of ammunition as recorded by the near sensors are shown below, primarily to illustrate the high degree of repeatability for shots of a given ammunition type, and the differences between different ammunition types.

The data shown below were recorded on 22 December 2016 at the Grafton County Fish and Game Association shooting range in Lebanon, New Hampshire, with an air temperature of -2°C , relative humidity of 95% and light snow falling throughout the duration of the experiment.

A. Fully Metal Jacketed (FMJ) Ammunition

The FMJ ammunition uses a 115 grain (7.45 g) projectile and typically achieves a mean projectile velocity, v_p , of 350 m s^{-1} at a range of 10 m. This ammunition type produced the largest muzzle blast and projectile charge transients observed in this study. The FMJ muzzle blast is positively charged as shown in Fig. 2.

B. Metal Jacketed Hollow Point (JHP) Ammunition

JHP ammunition has a 115 grain (7.45 g) projectile and typically achieves v_p of 350 m s^{-1} at a range of 10 m. The muzzle blast charge for this type of ammunition is complicated, but predominantly negative and only 33% of the amplitude of FMJ ammunition.

C. Metal Jacketed Hollow Point "HS" (JHP-HS) Ammunition

JHP-HS ammunition has a 124 grain (8.03 g) projectile and typically achieves v_p of 335 m s^{-1} at a range of 10 m. The muzzle blast charge for this type of ammunition is also complicated, but predominantly negative and approximately 40% of the amplitude of FMJ ammunition.

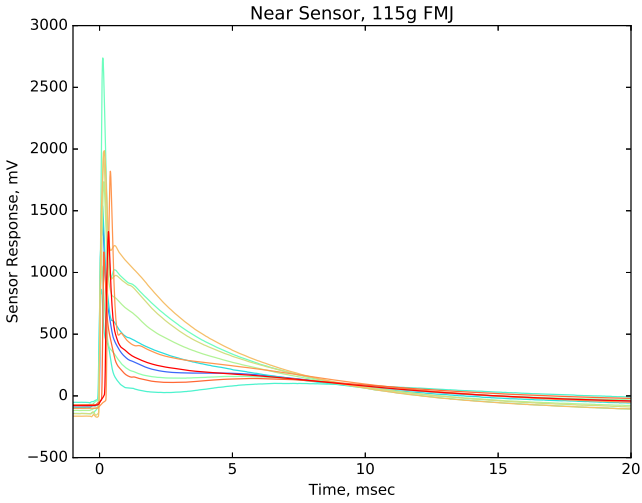


Fig. 2. Near sensor responses to 15 shots of FMJ ammunition. The charge transient associated with the muzzle blast is large and positive, likely obscuring any signal from the projectile.

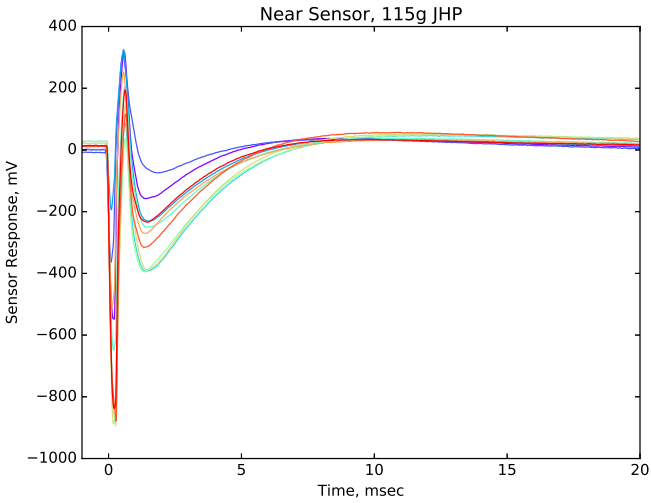


Fig. 3. Near sensor response for 10 shots of JHP ammunition.

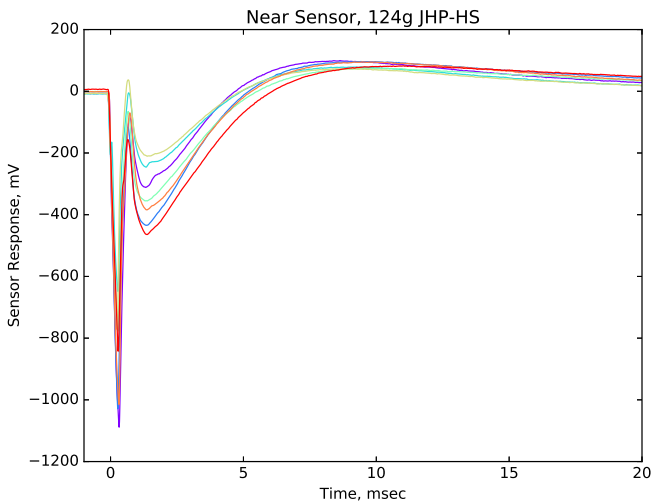


Fig. 4. Near sensor responses for 7 shots of JHP-HS ammunition

D. Materials Analysis

Many modern propellants are based on nitrocellulose with carefully engineered surface areas. Because these propellants only burn on the surface, the surface area of the propellant grain can help to control the rate of combustion and thus the maximum pressure achieved within the firing chamber [8].

Prior to burning, our propellant grains had a roughly spherical shape and diameters of approximately $900\ \mu\text{m}$, and appear to be a porous nitrocellulose structure with some inclusions (see Fig. 5).

After burning, the propellant debris featured three distinct particle types (see Fig. 6):

- 1) large ($50\ \mu\text{m}$ or more), smooth, macroporous particles
- 2) smaller ($30\ \mu\text{m}$ or less), irregular shaped, microporous particles
- 3) numerous μm and sub- μm fragments of types 1 and 2.

Both particle types 1 and 2 are discussed and shown in [9] and [10], suggesting that the particle types we observed are typical, and would be common to most propellant manufacturers.

IV. DISCUSSION

A point of considerable interest are the significant differences in polarity, duration, and time evolution of muzzle blast transients that exist between the three ammunition types. All three types feature a sudden pulse just after $t = 0$: positive for FMJ and negative for the JHP types. Immediately following this is a slow decay back to zero voltage, with a

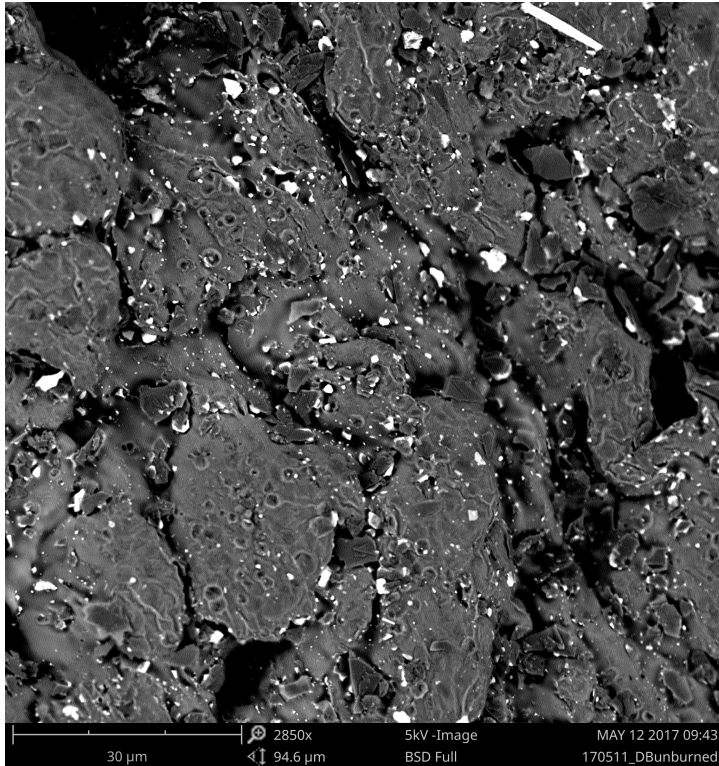


Fig. 5. Close up of the surface of an unburned propellant grain. The unburned grain has a typical diameter of $900\ \mu\text{m}$ and features a “wrinkled” surface with holes between 20 and $40\ \mu\text{m}$ across scattered over the surface. Both white (around $4\ \mu\text{m}$ maximum dimension, and containing Si and Al) and dark (harder to see, $8\ \mu\text{m}$ maximum dimension) structures are embedded in the grey matrix which is dominated by C and N, presumably the nitrocellulose.

relaxation time on the order of a few ms, again, positive for FMJ and mainly negative for the JHP ammunition types. This relaxation of the muzzle blast charge may be due to charge recombination and charge cloud dilution in the air. It is unclear if the projectile charge has any detectable impact on the recorded data in Figures 2, 3, and 4 or if it is simply overwhelmed by the much larger charges associated with the muzzle blast.

The muzzle blast transients appear to be highly repeatable, despite some variations in amplitude, and sufficiently unique that the signature of a specific ammunition type can be identified by inspection of the transient. This uniqueness is remarkable considering that the primer and propellant used by all three ammunition types is *identical*.

The muzzle blast signature evolution in time is likely caused by a number of interrelated phenomena, including gas-particulate flows, particle size and chemistry distributions

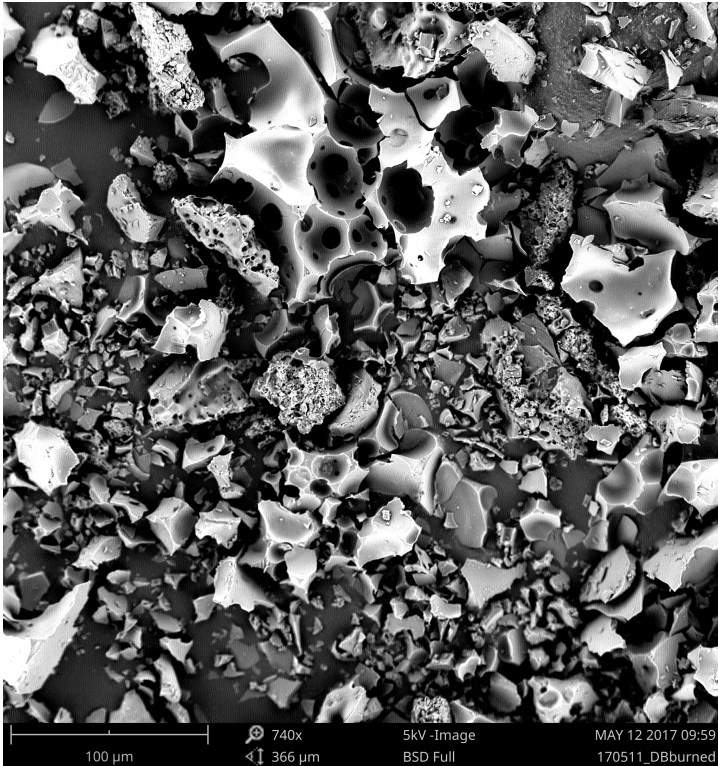


Fig. 6. Debris from burned propellant grain. The debris features three distinct types of particle: (1) large, smooth, macroporous structures, (2) smaller, rough, microporous structures, and (3) numerous μm and sub- μm fragments of both.

(which may be changing as a function of combustion time), propellant burn rates, and differences in the chemical and surface states between the particulates and the weapon barrel, and those of the projectile itself. The materials analysis presented here is but a small step towards better understanding the particulate loading of the dynamic gas-solids flow produced when firing a firearm.

This leaves us with few possible explanations for observed differences in muzzle blast charge transients between ammunition types. Clearly, the shape of the projectiles are different between the FMJ and hollow point types, but the materials for the projectile core and jacketing, and that of the cartridge itself are all identical. Normal manufacturing variations in projectile setback (i.e. the depth with which the back of the projectile is seated into the cartridge) may explain some of the amplitude variability from shot to shot of the *same* ammunition type, but seems unlikely to explain the difference in charge transients across different ammunitions. The ways in which the projectile shape affects

interactions between the gas-solids flow between the weapon barrel and the projectile itself, and how these flows translate into such different charge transients measured near the muzzle are all open questions at this time.

ACKNOWLEDGMENT

We gratefully acknowledge funding of this work through the U.S. Army Basic Research Program (6.1/T14). Permission to publish was granted by Director, Cold Regions Research and Engineering Laboratory.

REFERENCES

- [1] J. L. T. Haseborg and H. Trinks, "Electric charging and discharging processes of moving projectiles," *IEEE Transactions on Aerospace and Electronic Systems*, vol. AES-16, no. 2, pp. 227–232, March 1980.
- [2] —, "Detection of projectiles by electric field measurements," *IEEE Transactions on Aerospace and Electronic Systems*, vol. AES-16, no. 6, pp. 750–754, Nov 1980.
- [3] S. Vinci, J. Zhu, and D. Hull, "Analysis of electrostatic charge on small-arms projectiles," Proceedings of the SPIE, p. 83820M, 2012.
- [4] M. A. Noras, S. P. Ramsey, and B. B. Rhoades, "Projectile detection using quasi-electrostatic field sensor array," *Journal of Electrostatics*, vol. 71, no. 3, pp. 220 – 223, 2013.
- [5] C. J. Benfield, W. B. Williams, and M. Noras, "Application of novel quasi-electrostatic sensor arrays for time based data collection and processing of supersonic, subsonic, and transonic revolving projectiles," Proceedings of the SPIE, pp. 91 030H–91 030H–8, 2014.
- [6] D. Breton, N. Lamie, and E. Asenath-Smith, "Triboelectric charge variability in firearm particulates and projectiles," 2017, submitted to Journal of Electrostatics.
- [7] A. Savitzky and M. J. Golay, "Smoothing and differentiation of data by simplified least squares procedures." *Analytical Chemistry*, vol. 36, no. 8, pp. 1627–1639, 1964.
- [8] H. Miyauchi, M. Kumihashi, and T. Shibayama, "The contribution of trace elements from smokeless powder to post firing residues," *Journal of Forensic Science*, vol. 43, no. 1, pp. 90–96, 1998.
- [9] J. Lebieczik and D. L. Johnson, "Rapid search and quantitative analysis of gunshot residue particles in the SEM," *Journal of Forensic Science*, vol. 45, no. 1, pp. 83–92, 2000.
- [10] Z. Brożek-Mucha, "Chemical and morphological study of gunshot residue persisting on the shooter by means of scanning electron microscopy and energy dispersive x-ray spectrometry," *Microscopy and Microanalysis*, vol. 17, no. 06, pp. 972–982, 2011.